Biochemical and Biophysical Research Communications 433 (2013) 408–414

Contents lists available at SciVerse ScienceDirect

Biochemical and Biophysical Research Communications

journal homepage: www.elsevier.com/locate/ybbrc

Hydrogen peroxide impairs autophagic flux in a cell model of nonalcoholic fatty liver disease

Pengtao Jiang [a,c], Zhen Huang [b], Hong Zhao [b,*], Taotao Wei [a,*]

[a] National Laboratory of Biomacromolecules, Institute of Biophysics, Chinese Academy of Sciences, 15 Datun Road, Chaoyang District, Beijing 100101, PR China
[b] Department of Abdominal Surgical Oncology, Cancer Hospital, Chinese Academy of Medical Sciences, 17 Panjiayuan Nanli, Chaoyang District, Beijing 100021, PR China
[c] University of Chinese Academy of Sciences, 19 Yuquan Road, Shijingshan District, Beijing 100049, PR China

ARTICLE INFO

Article history:
Received 17 February 2013
Available online 26 March 2013

Keywords:
Nonalcoholic fatty liver disease
Autophagy
Reactive oxygen species
TNF-α

ABSTRACT

Nonalcoholic fatty liver disease (NAFLD) has become the leading cause of chronic liver disease, but the pathogenesis of NAFLD is not fully clear. The aim of this study was to determine whether autophagy plays a role in the pathogenesis of NAFLD. We found that the levels of autophagy were elevated in hepatoma cells upon exposure to free fatty acids, as confirmed by the increase in the number of autophagosomes. However, exposure of hepatoma cells to H_2O_2 and TNF-α, two typical "second hit" factors, increased the initiation of autophagy but inhibited the autophagic flux. The inhibition of autophagy sensitized cells to pro-apoptotic stimuli. Taken together, our results suggest that autophagy acts as a protective mechanism in the pathogenesis of NAFLD and that impairment of autophagy might induce more severe lesions of the liver. These findings will be a benefit to the understanding of the pathogenesis of NAFLD and might suggest a strategy for the prevention and cure of NAFLD.

1. Introduction

Exposure to fat-rich and fiber-poor diets disrupts metabolic homeostasis and causes elevated levels of circulating free fatty acids (FFAs) in humans, which will lead to the accumulation of triglycerides (TG) in hepatocytes [1,2]. Hepatic injury may occur when the capacity of hepatocytes to safely store excess FFA in form of TGs in lipid droplets is exceeded, causing non-alcoholic fatty liver disease (NAFLD) [3]. NAFLD has emerged as a considerable public health problem worldwide [4,5]. A significant number of NAFLD patients progress to non-alcoholic steatohepatitis (NASH), which leads to liver fibrosis and finally cirrhosis [6]. Once cirrhosis has developed, the mortality rate increases significantly due to a high risk of hepatic decompensation and hepatocellular carcinoma [7,8]. Understanding the molecular mechanisms of NAFLD is not only of biomedical and public health interest but also key to developing new avenues for specific treatment interventions.

Recently, it has been reported that autophagy is up-regulated during the progression of NAFLD. Autophagy occurs at low basal levels in all cells and is required for homeostasis of biomacromolecules. Autophagy can also be activated as an adaptive catabolic process in response to different forms of metabolic stress, including nutrient deprivation, growth factor depletion, hypoxia, and the accumulation of intracellular protein aggregates or lipids. This bulk form of degradation generates free amino and fatty acids that can be recycled within the organism. Once the autophagy balance in cells is disrupted, the adaptive role of autophagy in response to stress will be lost, which can ultimately result in many diseases [9]. For example, the accumulation of misfolded proteins in neurons causes neurodegenerative diseases, and defects of autophagy impair the clearance of misfolded proteins and accelerate the progress of neurodegeneration [10]. Autophagy also plays a role in tumor pathogenesis [11]. In hepatocytes, the inhibition of autophagy leads to significant accumulation of intracellular lipids [12], suggesting the possible involvement of autophagy in NAFLD-related diseases.

During the progression of NAFLD, the overloading of intracellular lipids by free fatty acid exposure is the "first hit", which will initiate the over-production of "second hit" factors, such as reactive oxygen species and proinflammatory cytokines [13,14]. These pathological factors may disrupt the initiation and execution of autophagy in different cell types [15–19]. However, their effects on autophagy in cell models of NAFLD remain unclear. In this study, we explored the relationship between autophagy and oxidative stress in NAFLD cell models. We found that oxidative stress

Abbreviations: NAFLD, nonalcoholic fatty liver disease; FFA, free fatty acid; TG, triglycerides; PA, palmitic acid; OA, oleic acid; BAF, bafilomycin A1; 3-MA, 3-methyladenine; AcD, Actinomycin D.

* Corresponding authors. Fax: +86 10 6770 9001 (H. Zhao), fax: +86 10 6487 1293 (T. Wei).
E-mail addresses: zhaohong9@sina.com (H. Zhao), weitt@moon.ibp.ac.cn (T. Wei).

0006-291X/$ - see front matter © 2013 Elsevier Inc. All rights reserved.
http://dx.doi.org/10.1016/j.bbrc.2013.02.118

potentiates the initiation of autophagy via activation of AMPK/ULK1-related mechanisms, but decreases autophagic flux by inhibiting the fusion between autophagosomes and lysosomes. The down-regulated levels of autophagy may play an important role in the potentiation of cell death induced by pro-apoptotic stimuli in hepatoma cells.

2. Materials and methods

2.1. Cells and reagents

RH-35 rat hepatoma cells and HepG2 human hepatoma cells were obtained from CTCC (Shanghai, China) and maintained in Dulbecco's modified Eagle medium (DMEM; Life Technologies, Grand Island, NY, USA) supplemented with 10% fetal bovine serum (FBS; Life Technologies). Palmitic acid (PA) and oleic acid (OA) were purchased from Sigma–Aldrich (St. Louis, MO, USA); TNF-α was purchased from Peprotech (Rocky Hill, NJ, USA); 3-methyladenine (3-MA) and bafilomycin A1 (BAF) were purchased from Merck-Millipore (Darmstadt, Germany); CCK-8 was purchased from DOJINDO (Kumamoto, Japan); Anti-LC3 was purchased from MBL (Nagoya, Japan); anti-actin and anti-ULK1 were purchased from Sigma–Aldrich; anti-phospho-AMPK, anti-AMPK, anti-phospho-ULK1, anti-phospho-mTOR, anti-mTOR and anti-Beclin-1 were from Cell Signaling Technology (Danvers, MA, USA); pEGFP-LC3 was kindly provided by Prof. Li Yu (Tsinghua University, Beijing, China). Other reagents were manufactured in China and were of analytical grade.

2.2. Nile Red staining and determination of intracellular lipid accumulation

RH-35 or HepG2 cells were incubated with 300 μM oleic acid (OA) plus 300 μM palmitic acid (PA) for 24 h. To visualize the intracellular lipid droplets, cells cultured on glass coverslips were stained with Nile Red (2 μg/ml; Life Technologies) for 20 min at 37 °C. Images were acquired with an Olympus FV500 laser scanning confocal microscope using an excitation wavelength of 488 nm and an emission wavelength of 550 nm. The intracellular triglyceride (TG) content was quantified with a commercially available kit (Biosino, Beijing, China) and normalized by protein content.

2.3. Plasmid transfection and confocal microscopy

RH-35 (1.5×10^6) or HepG2 (1×10^6) cells were resuspended in 100 μl of Amaxa nucleofection buffer (solution V; Amaxa Biosystems, Cologne, Germany) and mixed with 2 μg of the pEGFP-LC3 vector. This suspension was transferred to a sterile cuvette and treated using programs T-030 (RH-35) and T-028 (HepG2) on an Amaxa Nucleofector II device. After recovery for 30 min in complete DMEM medium, the cells were plated on glass coverslips, cultured for 24 h, and then incubated with 300 μM OA plus 300 μM PA for additional 24 h. The intracellular EGFP-LC3 fusion protein was visualized with an Olympus FV500 laser scanning confocal microscope using an excitation wavelength of 488 nm and an emission wavelength of 518 nm for EGFP.

2.4. Immunofluorescence

RH-35 and HepG2 cells were grown on glass coverslips and incubated with 300 μM OA plus 300 μM PA for 24 h, treated with hydrogen peroxide (100 μM) or TNF-α (20 ng/ml) plus AcD (0.2 μM) for 6 h, and fixed in 4% paraformaldehyde in phosphate-buffered saline (PBS) containing 1 mM EGTA and 3 mM $MgSO_4$. Cells were permeabilized with 0.2% triton X-100 in PBS at 37 °C for 10 min and blocked for 1 h at room temperature with PBS containing 5% goat serum albumin, 5% glycerol, and 0.04% sodium azide. After incubation with primary antibodies against LC3 in blocking buffer at 4 °C overnight, cells were washed three times with PBS, incubated with FITC-conjugated second antibody and DAPI (10 μg/ml) in blocking buffer for 1 h at 37 °C, and imaged with an Olympus FV500 laser scanning confocal microscope using an excitation wavelength of 488 nm and an emission wavelength of 518 nm. In some experiments, the lysosomes were labeled with LysoTracker Red (50 nM; Life Technologies).

2.5. Immunoblot analysis

RH-35 and HepG2 cells were incubated with 300 μM OA plus 300 μM PA for 24 h, treated with hydrogen peroxide (40 μM) or TNF-α (20 ng/ml) plus Actinomycin D (AcD; 0.2 μM) for indicated intervals, and lysed in lysis buffer [Tris–HCl 50 mM, Triton X-100 1%, sodium deoxycholate 0.2%, SDS 0.1%, NaCl 150 mM, 1× protease inhibitor cocktail (Merck-Millipore, Darmstadt, Germany)] at 4 °C. The lysates were centrifuged at 15,000×*g* for 10 min, and the concentration of the proteins in each lysate was determined with a Pierce BCA Kit (Rockford, IL, USA). Samples were resolved by 10% SDS–PAGE, transferred to polyvinylidene fluoride (PVDF) membranes, and blotted with proper primary antibodies. They were then incubated with appropriate peroxidase-conjugated secondary antibodies, and visualized using a chemiluminescent substrate (ECL; Perkin Elmer, Beijing, China) with Fuji SuperRX film (Tokyo, Japan).

2.6. Cell viability detection

Cells viability was detected by CCK-8 based on the reduction of 2-(2-Methoxyl-4-nitrophenyl)-3-(4-nitrophenyl)-5-(2,4-disulfonicacid benzene)-2H-tetrazolium sodium to a highly water-soluble formazan dye by mitochondrial dehydrogenase. RH-35 or HepG2 cells were seeded into 96-multiwell plates and then incubated with or without 300 μM OA plus 300 μM PA for 24 h. Cells were then treated with different concentrations of H_2O_2 (25, 50, 100, and 200 μM, respectively) at 37 °C for 24 h. CCK-8 was then added to each well, and cells were incubated for an additional 2 h. The absorbance of each well was recorded at 450 nm with a Thermo Fisher Multiskan MK3 microplate reader (Logan, UT, USA).

2.7. Data analysis

All data are expressed as the mean ± SD unless otherwise indicated. Differences between groups were compared by analysis of variance followed by ANOVA tests. Differences were considered to be statistically significant at $p < 0.05$.

3. Results and discussion

3.1. The number of autophagosomes was increased after free fatty acids exposure

To investigate the relationship between autophagy and NAFLD at the cellular level, we first established NAFLD cell models by incubating rat RH-35 and human HepG2 hepatoma cells with free fatty acids, according to previously described protocols [20]. Incubation of cells with 300 μM oleic acid (OA; a typical unsaturated fatty acid) plus 300 μM of the saturated fatty acid palmitic acid (PA; a typical saturated fatty acid) for 24 h induced significant steatosis, as confirmed by the formation of intracellular lipid droplets after Nile red staining (Fig. 1A). Quantification of intracellular TG further indicated the marked (>10-fold) accumulation of lipids in

cells incubated with OA/PA. In RH-35 cells treated with 300 μM OA plus 300 μM PA for 24 h, the intracellular TG concentration increased from 2.11 to 24.38 μg/mg. In HepG2 cells treated with 300 μM OA plus 300 μM PA for 24 h, the intracellular TG concentration increased from 1.32 to 19.21 μg/mg (Fig. 1B). However, the accumulation of intracellular lipids showed no effects on cell viability (Fig. 1C).

It has been reported that autophagy may be responsible for the elimination of excessive intracellular lipids in hepatocytes. We then investigated whether the levels of autophagy in hepatoma cells were affected after OA/PA exposure by monitoring the number of autophagosomes. The autophagy protein LC3 is a marker of autophagosomes in mammalian cells. Soon after its synthesis, nascent LC3 is processed at its C terminus by Atg4 and becomes LC3-I, which has a glycine residue at the C-terminal end. LC3-I is subsequently conjugated with phosphatidylethanolamine (PE) to become LC3-II (LC3-PE) by a ubiquitination-like enzymatic reaction. In contrast to the cytoplasmic localization of LC3-I, LC3-II

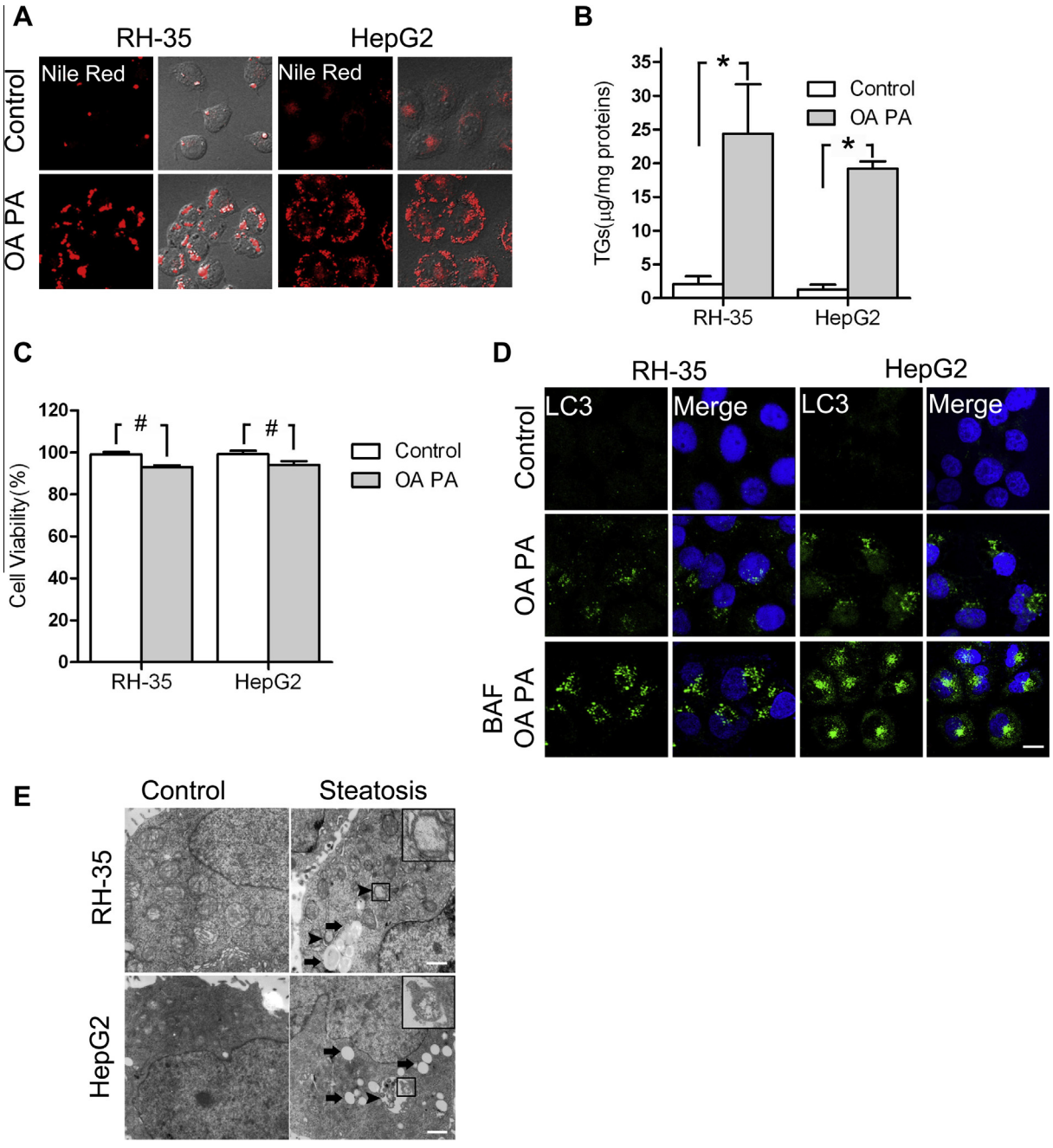

Fig. 1. Exposure to free fatty acids increased the number of autophagosomes. (A) Accumulation of intracellular lipid droplets in RH-35 and HepG2 cells treated with free fatty acids. RH-35 and HepG2 cells were incubated with OA (300 μM) plus PA (300 μM) for 24 h, stained with Nile Red (1 μg/ml) for 10 min and viewed on an Olympus inverted laser scanning confocal microscope. (B) Quantification of intracellular lipids. RH-35 and HepG2 cells were incubated with OA (300 μM) plus PA (300 μM) for 24 h and the intracellular triglyceride (TG) content was determined. Values are mean ± SD ($n = 3$; $^*p < 0.05$). (C) Accumulation of intracellular lipids shows no effects on the cell viability. RH-35 and HepG2 cells were incubated with OA (300 μM) plus PA (300 μM) for 24 h and cell viability was detected by CCK-8. Values are mean ± SD ($n = 8$; #, $p > 0.05$). (D) The number of autophagosomes was increased after exposure to free fatty acids. RH-35 and HepG2 cells were incubated with OA (300 μM) plus PA (300 μM) for 24 h and intracellular autophagosomes were observed after immunofluorescent staining with anti-LC3 antibody. Scale bars: 10 μm. (E) The ultrastructure of RH-35 and HepG2 cells after free fatty acids exposure. RH-35 and HepG2 cells were incubated with OA (300 μM) plus PA (300 μM) for 24 h and the ultrastructure was examined by transmission electron microscopy. Arrowheads denote autophagosomes. Arrows denote lipid droplets. Scale bar: 1 μm. (For interpretation of the references to color in this figure legend, the reader is referred to the web version of this article.)

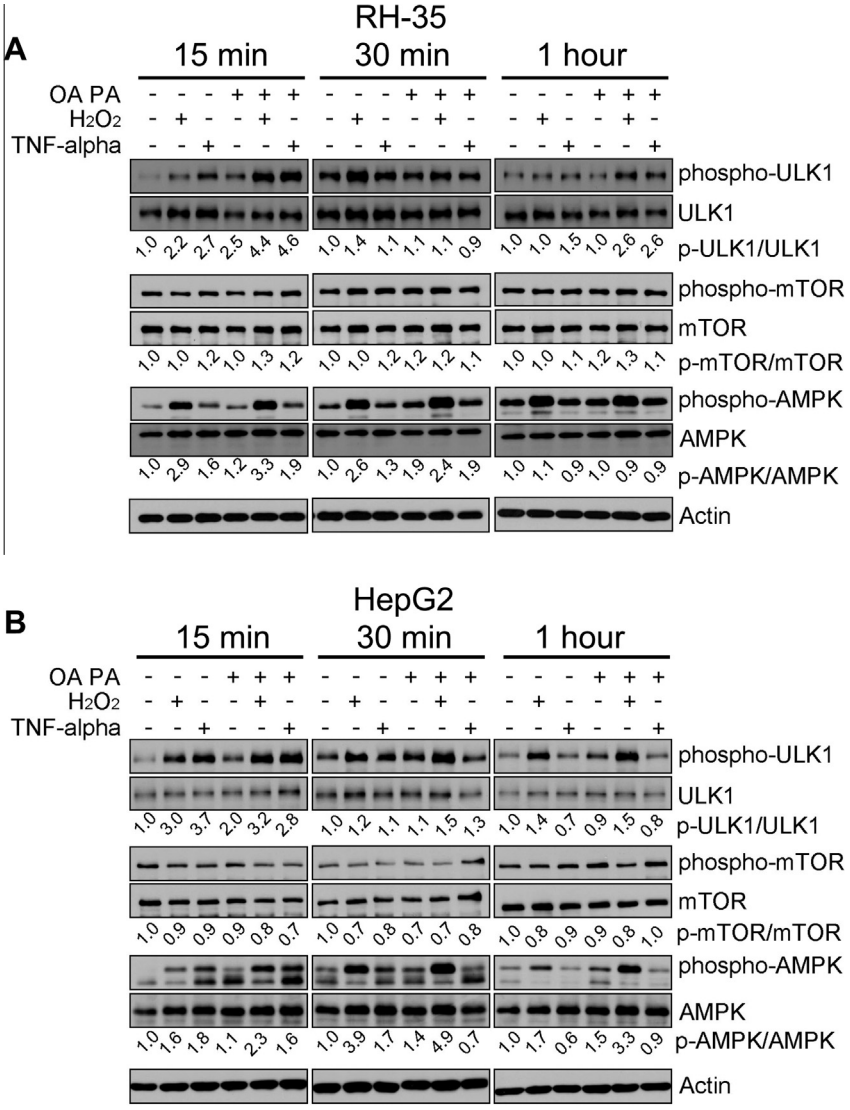

Fig. 2. H_2O_2 treatment increased the initiation of autophagy. (A) H_2O_2 treatment activates the AMPK/ULK1 signaling pathway in RH-35 cells. RH-35 cells were incubated with OA (300 μM) plus PA (300 μM) for 24 h and then exposed to hydrogen peroxide (40 μM) or TNF-α (20 ng/ml) plus AcD (0.2 μM) for 15 min, 30 min, or 1 h. The levels of phospho-ULK1, total ULK1, phospho-mTOR, total mTOR, phospho-AMPK and total AMPK levels were determined with proper antibodies and the density of each band was quantified. (B) H_2O_2 treatment activates the AMPK/ULK1 signaling pathway in HepG2 cells. HepG2 cells were incubated with OA (300 μM) plus PA (300 μM) for 24 h and then exposed to hydrogen peroxide (40 μM) or TNF-α (20 ng/ml) plus AcD (0.2 μM) for 15 min, 30 min, or 1 h. The levels of phospho-ULK1, total ULK1, phospho-mTOR, total mTOR, phospho-AMPK and total AMPK levels were determined with proper antibodies and the density of each band was quantified.

associates with both the outer and inner membranes of the autophagosome. Thus, endogenous LC3 or GFP-LC3 is visualized by fluorescence microscopy either as a diffuse cytoplasmic pool or as punctate structures that primarily represent autophagosomes. We observed a low level of basal autophagy in control cells, as indicated by the low number of LC3 puncta (Fig. 1D). However, when the cells were exposed to 300 μM OA plus 300 μM PA for 24 h, the number of LC3 puncta was increased drastically. Pretreatment of cells with bafilomycin A1 (BAF; a V-ATPase inhibitor which prevents the degradation of autophagosomes) further increased the number of intracellular LC3 puncta, suggesting a drastic increase in autophagic flux after exposure of cells to free fatty acids.

To ascertain the increase in autophagy after free fatty acid exposure, we observed the accumulation of intracellular autophagosomes directly with transmission electron microscopy. As clearly indicated in Fig. 1E, treatment of RH-35 and HepG2 cells with OA/PA enhanced the formation of autophagosomes. After OA/PA treatment, cells accumulated many lipid droplets (indicated by arrows), and autophagosomes showed massive vacuolization of the cytoplasm (indicated by arrowheads).

3.2. H_2O_2 treatment increased the initiation of autophagy

According to the classical "two-hit" hypothesis of the progression of NAFLD, the overloading of intracellular lipids by free fatty acid exposure is the "first hit", which will initiate the over-production of reactive oxygen species and proinflammatory cytokines. These factors act as the "second hit" and induce damage to the liver [13]. To mimic the liver damage at the cellular levels, we incubated the OA/PA-treated hepatoma cells with H_2O_2 or TNF-α (two typical factors often overproduced in the progression of NAFLD [20,21]), and then determined the effect on autophagy by analyzing the kinetics of autophagy-related pathways. Because ULK1 plays a central role in the initiation of autophagy [22], we first analyzed both phospho-ULK1 and total ULK1 levels in hepatoma cells. As clearly indicated in Fig. 2A, the phospho-ULK1 levels increased

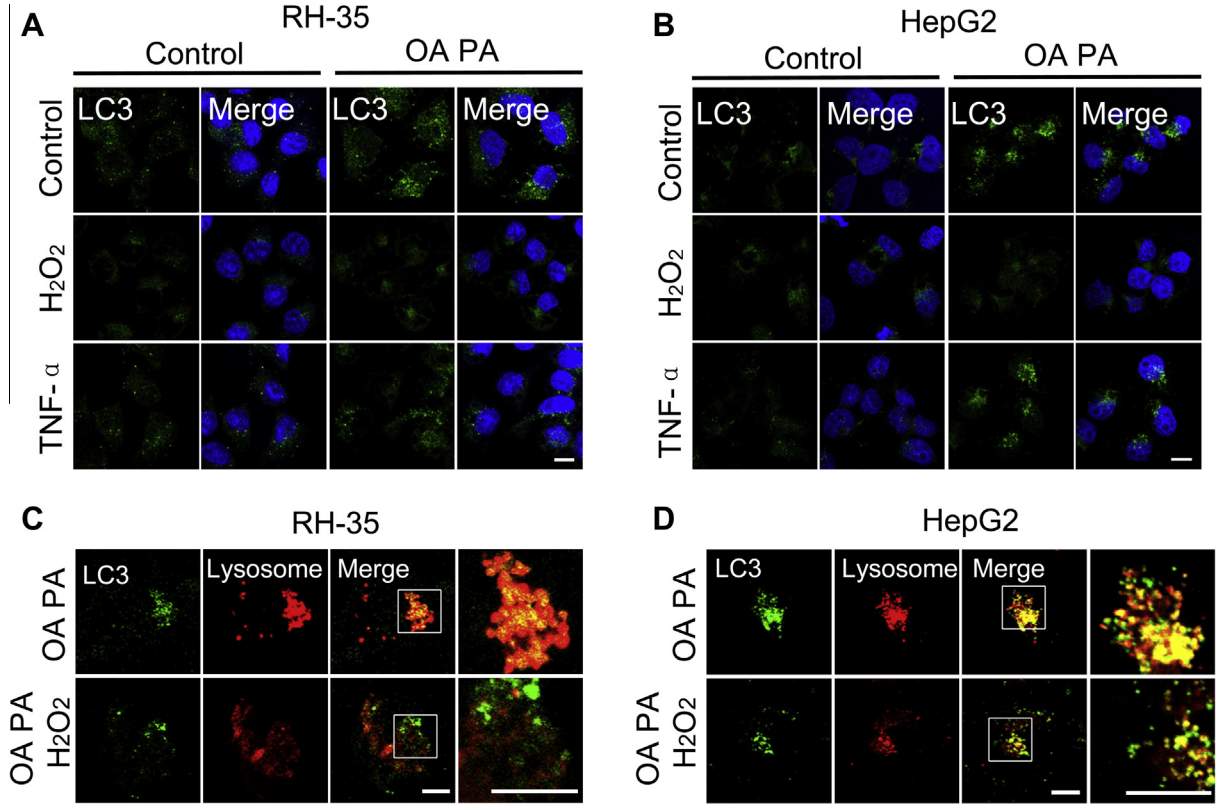

Fig. 3. H_2O_2 treatment decreased the number of autophagosomes and impaired fusion between autophagosomes and lysosomes. (A) H_2O_2 treatment decreased the number of autophagosomes in RH-35 cells. RH-35 cells were incubated with OA (300 μM) plus PA (300 μM) for 24 h and then exposed to hydrogen peroxide (40 μM) or TNF-α (20 ng/ml) plus AcD (0.2 μM) for 4 h. Intracellular autophagosomes were observed after immunofluorescent staining with anti-LC3 antibody. Scale bars: 10 μm. (B) H_2O_2 treatment decreased the number of autophagosomes in HepG2 cells. HepG2 cells were incubated with OA (300 μM) plus PA (300 μM) for 24 h and then exposed to hydrogen peroxide (40 μM) or TNF-α (20 ng/ml) plus AcD (0.2 μM) for 4 h. Intracellular autophagosomes were observed after immunofluorescent staining with anti-LC3 antibody. Scale bars: 10 μm. (C) H_2O_2 treatment impaired the fusion between autophagosomes and lysosomes in RH-35 cells. RH-35 cells were transfected with pEGFP-LC3 plasmid by Nucleofection™, incubated with OA (300 μM) plus PA (300 μM) for 24 h, and then exposed to hydrogen peroxide (40 μM) for 2 h. Lysosome-related vesicles were labeled with LysoTracker Red (50 nm) and cells were visualized using a confocal microscope. Scale bar: 10 μm. (D) H_2O_2 treatment impaired the fusion between autophagosomes and lysosomes in HepG2 cells. HepG2 cells were transfected with pEGFP-LC3 plasmid by Nucleofection™, incubated with OA (300 μM) plus PA (300 μM) for 24 h, and then exposed to hydrogen peroxide (40 μM) for 2 h. Lysosome-related vesicles were labeled with LysoTracker Red (50 nm) and cells were visualized using a confocal microscope. Scale bar: 10 μm. (For interpretation of the references to color in this figure legend, the reader is referred to the web version of this article.)

rapidly after the addition of H_2O_2 or TNF-α, suggesting the activation of the ULK1 kinase pathway by these factors. Similar results were also obtained in HepG2 human hepatoma cells, as shown in Fig. 2B.

Because ULK1 can be directly activated by either AMPK or mTOR [23], we sought to determine which of these two kinases was responsible for the H_2O_2 or TNF-α-dependent activation of ULK1. We determined the phospho-AMPK and phospho-mTOR levels in RH-35 rat hepatoma cells and found that the phospho-AMPK levels were significantly increased 15 min after H_2O_2 or TNF-α exposure, suggesting the activation of the AMPK signaling pathway. In contrast, the cellular levels of phospho-mTOR remained unchanged. These results suggested that AMPK, rather than mTOR, was involved in H_2O_2 or TNF-α-induced activation of ULK1, and initiation of autophagy in hepatoma cells.

3.3. H_2O_2 treatment decreased the number of autophagosomes and impaired the fusion of autophagosomes and lysosomes

Having demonstrated that H_2O_2 or TNF-α exposure induced the activation of the AMPK/ULK1 kinase pathway, which may promote the initiation of autophagy in hepatoma cells, we next evaluated the effects of H_2O_2 or TNF-α on the formation of autophagosomes. Immunofluorescence analysis of LC3 localization indicated that the number of autophagosomes was significantly decreased in both RH-35 and HepG2 hepatoma cells treated with H_2O_2, as shown in Fig. 3A and B. TNF-α treatment also decreased the number of autophagosomes to some extent. To further monitor the intracellular localization of LC3, cells were transfected with an EGFP-LC3 vector. Confocal images clearly indicated that in both RH-35 rat hepatoma cells and HepG2 human hepatoma cells preincubated with OA/PA, the GFP-LC3-harboring puncta co-localized with LysoTracker, a marker for lysosome-like vesicles, indicating the formation of autolysosomes as a result of fusion between autophagosomes and lysosomes (Fig. 3C and D; upper panel). However, when OA/PA-treated cells were incubated with H_2O_2, the GFP-LC3-harboring puncta showed only partial co-localization with LysoTracker (Fig. 3C and D; lower panel), suggesting that H_2O_2 treatment impaired the fusion between autophagosomes and lysosomes.

3.4. H_2O_2 treatment inhibited autophagic flux

The above data suggested that H_2O_2 treatment up-regulated the initiation of autophagy, but decreased the numbers of autophagosomes in OA/PA-treated hepatoma cells. However, the initiation and execution of autophagy machinery in mammalian cells is a highly dynamic process. The observed decrease in the numbers of autophagosomes might be due to either decreased formation or accelerated turnover [9]. We therefore analyzed autophagic flux by incubating cells with bafilomycine A1 (BAF), which blocked the

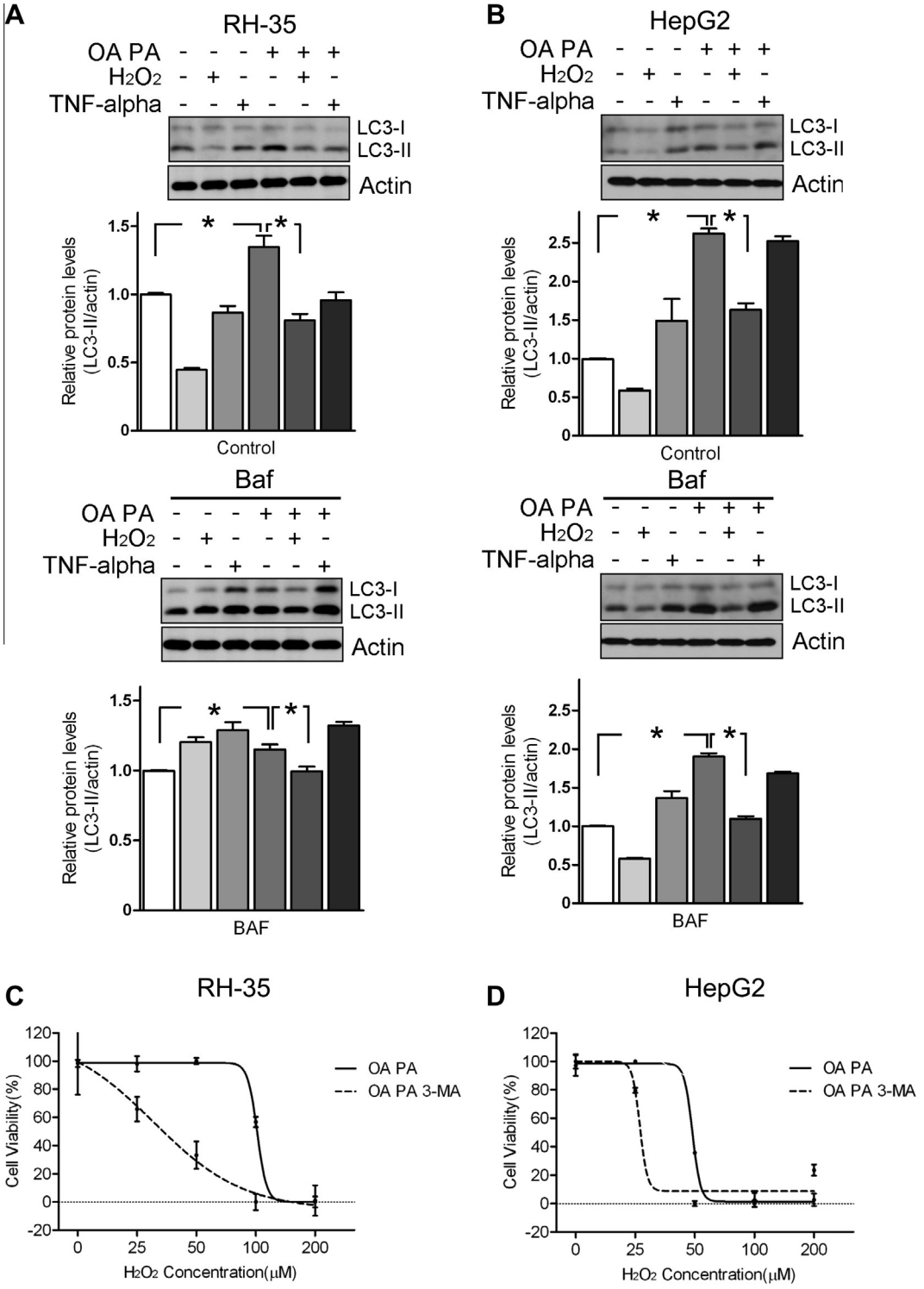

Fig. 4. H_2O_2 treatment inhibited autophagic flux. (A) H_2O_2 treatment inhibited autophagic flux in RH-35 cells. RH-35 cells were incubated with OA (300 μM) plus PA (300 μM) for 24 h and then exposed to hydrogen peroxide (40 μM) or TNF-α (20 ng/ml) plus AcD (0.2 μM) for 4 h in the presence or absence of 50 nm bafilomycin A1. The levels of LC3-I and -II were determined by immunoblot and typical results with the corresponding densitometry analysis are shown. Values are mean ± SD ($n = 3$; $^*p < 0.05$). (B) H_2O_2 treatment inhibited autophagic flux in HepG2 cells. HepG2 cells were incubated with OA (300 μM) plus PA (300 μM) for 24 h and then exposed to hydrogen peroxide (40 μM) or TNF-α (20 ng/ml) plus AcD (0.2 μM) for 4 h in the presence or absence of 50 nm bafilomycin A1. The levels of LC3-I and -II were determined by immunoblot and typical results with the corresponding densitometry analysis are shown. Values are mean ± SD ($n = 3$; $^*p < 0.05$). (C) Inhibition of autophagy sensitized RH-35 cells to H_2O_2-induced cell death. RH-35 cells were incubated with OA (300 μM) plus PA (300 μM) for 24 h and then pretreated with 3-MA (1 mM) to inhibit autophagy. Cells were then exposed to H_2O_2 (0, 25, 50, 100 and 200 μM) for 12 h. Cell viability was determined by CCK-8. Values are mean ± SD ($n = 8$). (D) Inhibition of autophagy sensitized HepG2 cells to H_2O_2-induced cell death. HepG2 cells were incubated with OA (300 μM) plus PA (300 μM) for 24 h and then pretreated with 3-MA (1 mM) to inhibit autophagy. Cells were then exposed to H_2O_2 (0, 25, 50, 100 and 200 μM) for 12 h. Cell viability was determined by CCK-8. Values are mean ± SD ($n = 8$).

degradation of LC3, followed by the detection of cellular LC3-II and LC3-I protein levels by immunoblot. Results shown in Fig. 4A clearly indicated that, in comparison with control hepatoma cells, the level of cellular LC3-II was significantly increased in OA/PA pretreated cells ($^{*}p < 0.05$), suggesting that the exposure of hepatoma cells to free fatty acids markedly increased autophagic flux. However, when cells were treated with H_2O_2 or TNF-α, cellular LC3-II levels were significantly decreased ($^{*}p < 0.05$), suggesting a decrease in the formation of autophagosomes (LC3-harboring vesicles) and significant inhibition of autophagic flux in free fatty acids-treated hepatoma cells.

It is generally accepted that autophagy may play a pro-survival role in stressed cells [24,25]. Because our data suggested that H_2O_2 impaired autophagic flux in free fatty acid-treated hepatoma cells, we then asked whether the inhibition of autophagy might sensitize cells to H_2O_2-induced cell death. Pretreatment of hepatoma cells with 3-MA, which inhibited the autophagic machinery, significantly sensitized cells to H_2O_2-induced cell death. As shown in Fig. 4C, the EC_{50} of H_2O_2 in RH-35 cells was 101.7 μM; however, when cells were pretreated with 3-MA, the EC_{50} decreased to 30.33 μM. Similar results were also obtained in HepG2 cells. The EC_{50} of H_2O_2 in HepG2 cells decreased from 48.6 μM to 26.4 μM after 3-MA pretreatment, suggesting that the inhibition of autophagy sensitized hepatoma cells to cell death in cellular models of NAFLD.

Taken together, our results, provide direct evidence that exposure of hepatoma cells to free fatty acids (“first hit” factors of NAFLD) increased autophagy levels, which may play important role in “self-protection” against stress conditions. In the course of NAFLD progression, the elevated levels of H_2O_2 or TNF-α (“second hit” factors of NAFLD) might impair the execution of autophagic machinery and decrease autophagic flux, which would sensitize cells to proapoptotic stimuli. These findings will be a benefit to the understanding of NAFLD pathogenesis, and may lead to new strategies for the prevention and cure of NAFLD.

Acknowledgments

This work was supported by grants from the National Basic Research Program of China (Grants 2010CB833701 and 2012CB9 34003), the National Natural Science Foundation of China (Grants 31070736 and 81201967), and the Beijing Natural Science Foundation of China (Grant 7132193). The authors would like to thank Prof. Li Yu (Tsinghua University) for kindly providing the pEGFP-LC3 vector, and Wenmin Zhong and Yan Teng (Institute of Biophysics, CAS) for technical assistance.

References

[1] G. Marchesini, M. Brizi, G. Bianchi, S. Tomassetti, E. Bugianesi, M. Lenzi, A.J. McCullough, S. Natale, G. Forlani, N. Melchionda, Nonalcoholic fatty liver disease: a feature of the metabolic syndrome, Diabetes 50 (2001) 1844–1850.
[2] N. Mendez-Sanchez, M. Arrese, D. Zamora-Valdes, M. Uribe, Current concepts in the pathogenesis of nonalcoholic fatty liver disease, Liver Int. 27 (2007) 423–433.
[3] N. Kumashiro, D.M. Erion, D. Zhang, M. Kahn, S.A. Beddow, X. Chu, C.D. Still, G.S. Gerhard, X. Han, J. Dziura, K.F. Petersen, V.T. Samuel, G.I. Shulman, Cellular mechanism of insulin resistance in nonalcoholic fatty liver disease, Proc. Natl. Acad. Sci. USA 108 (2011) 16381–16385.
[4] J.D. Browning, L.S. Szczepaniak, R. Dobbins, P. Nuremberg, J.D. Horton, J.C. Cohen, S.M. Grundy, H.H. Hobbs, Prevalence of hepatic steatosis in an urban population in the United States: impact of ethnicity, Hepatology 40 (2004) 1387–1395.
[5] J.G. Fan, G.C. Farrell, Epidemiology of non-alcoholic fatty liver disease in China, J. Hepatol. 50 (2009) 204–210.
[6] M. Charlton, Nonalcoholic fatty liver disease: a review of current understanding and future impact, Clin. Gastroenterol. Hepatol. 2 (2004) 1048–1058.
[7] L.M. Grant, M. Lisker-Melman, Nonalcoholic fatty liver disease, Ann. Hepatol. 3 (2004) 93–99.
[8] J.M. Clark, F.L. Brancati, A.M. Diehl, Nonalcoholic fatty liver disease, Gastroenterology 122 (2002) 1649–1657.
[9] B. Levine, G. Kroemer, Autophagy in the pathogenesis of disease, Cell 132 (2008) 27–42.
[10] D.C. Rubinsztein, J.E. Gestwicki, L.O. Murphy, D.J. Klionsky, Potential therapeutic applications of autophagy, Nat. Rev. Drug Discovery 6 (2007) 304–312.
[11] B. Levine, Cell biology: autophagy and cancer, Nature 446 (2007) 745–747.
[12] M. Amir, M.J. Czaja, Autophagy in nonalcoholic steatohepatitis, Expert Rev. Gastroenterol. Hepatol. 5 (2011) 159–166.
[13] C.P. Day, O.F. James, Steatohepatitis: a tale of two “hits”?, Gastroenterology 114 (1998) 842–845
[14] J.K. Dowman, J.W. Tomlinson, P.N. Newsome, Pathogenesis of non-alcoholic fatty liver disease, Q. J. Med. 103 (2010) 71–83.
[15] J. Huang, G.Y. Lam, J.H. Brumell, Autophagy signaling through reactive oxygen species, Antioxid. Redox Signaling 14 (2011) 2215–2231.
[16] R. Zhou, A.S. Yazdi, P. Menu, J. Tschopp, A role for mitochondria in NLRP3 inflammasome activation, Nature 469 (2011) 221–225.
[17] A. Ashkenazi, R.S. Herbst, To kill a tumor cell: the potential of proapoptotic receptor agonists, J. Clin. Invest. 118 (2008) 1979–1990.
[18] M. Djavaheri-Mergny, M.C. Maiuri, G. Kroemer, Cross talk between apoptosis and autophagy by caspase-mediated cleavage of Beclin 1, Oncogene 29 (2010) 1717–1719.
[19] G. Jia, G. Cheng, D.M. Gangahar, D.K. Agrawal, Insulin-like growth factor-1 and TNF-alpha regulate autophagy through c-jun N-terminal kinase and Akt pathways in human atherosclerotic vascular smooth cells, Immunol. Cell Biol. 84 (2006) 448–454.
[20] A.E. Feldstein, N.W. Werneburg, A. Canbay, M.E. Guicciardi, S.F. Bronk, R. Rydzewski, L.J. Burgart, G.J. Gores, Free fatty acids promote hepatic lipotoxicity by stimulating TNF-alpha expression via a lysosomal pathway, Hepatology 40 (2004) 185–194.
[21] C.P. Oliveira, L.C. da Costa Gayotto, C. Tatai, B.I. Della Bina, M. Janiszewski, E.S. Lima, D.S. Abdalla, F.P. Lopasso, F.R. Laurindo, A.A. Laudanna, Oxidative stress in the pathogenesis of nonalcoholic fatty liver disease, in rats fed with a choline-deficient diet, J. Cell Mol. Med. 6 (2002) 399–406.
[22] S. Alers, A.S. Loffler, S. Wesselborg, B. Stork, Role of AMPK-mTOR-Ulk1/2 in the regulation of autophagy: cross talk, shortcuts, and feedbacks, Mol. Cell Biol. 32 (2012) 2–11.
[23] J. Kim, M. Kundu, B. Viollet, K.L. Guan, AMPK and mTOR regulate autophagy through direct phosphorylation of Ulk1, Nat. Cell Biol. 13 (2011) 132–141.
[24] E.H. Baehrecke, Autophagy: dual roles in life and death?, Nat Rev. Mol. Cell Biol. 6 (2005) 505–510.
[25] J.M. Gump, A. Thorburn, Autophagy and apoptosis: what is the connection?, Trends Cell Biol 21 (2011) 387–392.